Hindawi
International Journal of Aerospace Engineering
Volume 2020, Article ID 8891051, 11 pages
https://doi.org/10.1155/2020/8891051

Research Article

Adaptive Backstepping Sliding Mode Control of Air-Breathing Hypersonic Vehicles

Shuo Wang, Ju Jiang, and Chaojun Yu

College of Automation Engineering, Nanjing University of Aeronautics and Astronautics, 211106 Nanjing, China

Correspondence should be addressed to Ju Jiang; jiangju@nuaa.edu.cn

Received 6 July 2020; Revised 28 August 2020; Accepted 9 September 2020; Published 17 September 2020

Academic Editor: Hao An

Copyright © 2020 Shuo Wang et al. This is an open access article distributed under the Creative Commons Attribution License, which permits unrestricted use, distribution, and reproduction in any medium, provided the original work is properly cited.

In this paper, a controller combining backstepping and adaptive supertwisting sliding mode control method is proposed for altitude and velocity tracking control of air-breathing hypersonic vehicles (AHVs). Firstly, the nonlinear longitudinal model of AHV is introduced and transformed into a strict feedback form, to which the backstepping method can be applied. Considering the longitudinal trajectory tracking control problem (altitude control and velocity control), the altitude tracking control system is decomposed to several one-order subsystems based on the backstepping method, and an adaptive supertwisting sliding mode controller is designed for each subsystem, in order to obtain the virtual control variables and actual control input. Secondly, the overall stability of the closed-loop system is proved by the Lyapunov stability theory. At last, the simulation is carried out on an AHV model. The results show that the proposed controller has good control performances and good robustness in the parameter perturbation case.

1. Introduction

An air-breathing hypersonic vehicle (AHV) as a kind of vehicle can cruise at a speed larger than 5 Mach in a near-space area. It has attracted much attention of researchers from all over the world because of its high military application value [1–3]. However, the flight control of AHV is still a challenging task. Considering the strong nonlinearity, coupling, parameter uncertainties, and external disturbances of AHV, the controller is required to be highly robust and have rapid response to the model uncertainties.

As far as we know, the modelling of AHV in most papers mainly relies on aerodynamic theory and CFD technology, and the lack of actual aerodynamic data of AHV in a near-space area can lead to inevitable modelling errors [4, 5]. Moreover, a large flight envelope leads to strong nonlinear characteristics of AHV. In addition, atmospheric disturbances change continuously during the whole flight process of AHV, which should not be ignored [6]. The above factors require the AHV controller to have strong robustness.

The strong nonlinearity of the AHV model makes the linear control methods difficult to be applied in the whole flight envelope. Although piecewise linear design and switching LPV system control [7, 8] were studied, which can ensure the stability of the controller in the whole flight envelope, the control performance is still limited. Therefore, nowadays, more nonlinear control methods [9–15] including input-output feedback linearization, sliding mode control, backstepping control, and fuzzy control have been employed on controller design of AHV to deal with the flight control problems.

Sliding mode control (SMC) has the advantage of remarkable robustness to parameter uncertainties, which can eliminate the influence of the matched uncertainties in control systems. However, there are some uncertainties which do not satisfy matching conditions; these unmatched uncertainties cannot be eliminated by SMC. In literature [16], the disturbance observer was used to estimate the uncertain part of the system and then eliminate the influence of disturbances. However, the accuracy of the disturbance observer is easily affected by system parameters, which leads to a decrease in tracking accuracy. In 2012, a new adaptive supertwisting sliding mode control [17] was proposed, which is suitable for the first-order nonlinear system and has a good

output chattering suppression performance. The control gain will change with external disturbances; in addition, the algorithm does not need the upper bound of disturbances, which is difficult to obtain in some cases.

Since 1991 [18], the backstepping method has become a hot research topic. It can be directly applied to nonlinear systems and has good performance in dealing with unmatched uncertainties. However, in the design of a backstepping controller, it is necessary to solve the multiple derivatives of the virtual control variable, which leads to the problem of "explosion of terms." Swaroop et al. proposed the dynamic surface (DSC) method to solve the problem effectively in 2000 [19]. The design idea is to use the first-order low-pass filter to calculate the differential of the virtual control variable. However, in order to reduce the system error, the filter period of DSC needs to be short enough, which increases the difficulty of DSC implementation.

Because the traditional backstepping method is not robust enough and the controller is conservative, some improved control methods have been proposed successively, including dynamic backstepping control [20, 21] and adaptive backstepping control [22]. The combination of backstepping and sliding mode control can effectively deal with the problems caused by matched uncertainties and unmatched uncertainties and can improve the robustness of the control system. In the first n-1 steps of backstepping, the controller designed in Reference [23] adopted adaptive backstepping to eliminate the influence of unmatched uncertainty of the system and the terminal sliding mode controller was designed. This backstepping sliding mode controller is robust to uncertain factors of the system and has fast convergence speed. In Reference [24], the backstepping control and terminal sliding mode control were combined to design the altitude and velocity controller of a hypersonic vehicle. The control performance is good, but the design of the sliding surface is too complex. Estrada et al. proposed a controller combining backstepping and high-order sliding modes [25], which can achieve finite-time tracking for MIMO systems with parametric uncertainties. Xia et al. designed an attitude controller for a missile model using the backstepping sliding mode method [26], which has good performance in attitude tracking control. In the controller design process, an extended state observer was applied to estimate lumped uncertainty.

In practical application, the hypersonic vehicle needs to fly in varying atmospheric environments, which will cause considerable parameter uncertainties and disturbances, especially during the climbing section. However, the method proposed above cannot deal with complex uncertainties with unknown upper bounds well. Therefore, in this paper, a novel control scheme based on adaptive backstepping sliding mode control is designed for AHVs with parameter uncertainties and external disturbances. The main contributions of this paper are summarized as follows.

(1) The proposed method can deal with both matched and unmatched uncertainties in the AHV model. Firstly, the AHV model is transformed into a velocity subsystem and altitude subsystem which have a strict feedback form. By applying the backstepping method, the controller is designed in a backward step-by-step way, which is suitable for dealing with unmatched uncertainties. In each step, the adaptive supertwisting sliding mode is designed to compensate uncertainties

(2) The application of the supertwisting sliding mode algorithm is extended by combining it with backstepping and parameter adaption. Combined with the backstepping method, the application of supertwisting is extended from first-order systems to high-order systems. The introduction of parameter adaption accommodates the unknown upper bounds of uncertainties

(3) The stability of the closed-loop system is theoretically analysed, and detailed simulations are carried out

The outline of this paper is organized as follows. In Section 2, the longitudinal dynamical model of an AHV is introduced; in order to apply the backstepping method, the nonlinear aircraft model is transformed into a strict feedback form. In Section 3, the backstepping sliding mode control scheme is proposed; then, controllers for altitude and velocity tracking are presented. In Section 4, system stability is analysed by the Lyapunov method. Numerical simulations are given in Section 5, and the conclusion is given in Section 6.

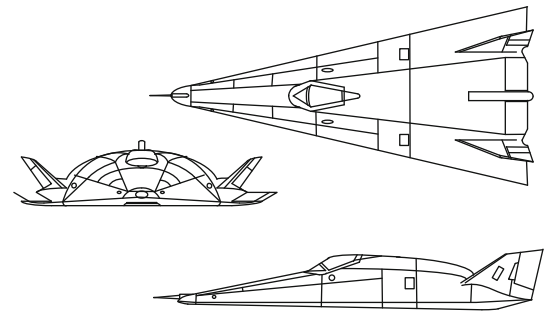

Figure 1: Configuration of hypersonic vehicle.

Table 1: Parameters of the AHV model.

Parameter	Value	Units
Mass	100200	kg
Airframe length	60.69	m
Reference area	369	m^2
Aerodynamic chord	30	m^2
Moment of inertia	8466900	$kg{\cdot}m^2$

2. Vehicle Model

2.1. Longitudinal Dynamic Model of AHV. The AHV studied in this paper is shown in Figure 1, which has a blended wing body with two elevators at the trailing edge of the wing. The data of the AHV model comes from an experimental aircraft model [27]. Some parameters of the AHV model are shown in Table 1.

The research objective of this paper is altitude and velocity tracking control. The longitudinal dynamic equations are as follows:

$$\begin{cases} \dot{V} = \dfrac{T\cos a - D}{m} - g\sin\gamma + d_V, \\ \dot{\gamma} = \dfrac{L + T\sin a}{mV} - \dfrac{g\cos\gamma}{V} + d_\gamma, \\ \dot{q} = \dfrac{M_y}{I_y} + d_q, \\ \dot{a} = q - \dot{\gamma}, \\ \dot{h} = V\sin\gamma, \end{cases} \tag{1}$$

where d_V, d_γ, and d_q represent the lumped uncertainties of velocity, flight path angle, and pitch angle rate equations, including parameter uncertainties, unmodelled dynamics, and external disturbances. V, γ, q, α, and h represent the velocity, flight path angle, pitching angle rate, angle of attack, and altitude of AHV. m, g, M_y, and I_y represent the mass, gravitational constant, pitching moment, and moment of inertia, respectively. For the lift L, drag D, and engine thrust T, we have

$$\begin{cases} L = \dfrac{1}{2}\rho V^2 s C_L, \\ D = \dfrac{1}{2}\rho V^2 s C_D, \\ T = \dfrac{1}{2}\rho V^2 s C_T, \\ C_m(\delta_e) = 0.0292(\delta_e - \alpha), \\ M_y = \dfrac{1}{2}\rho V^2 s\bar{c}(C_m + C_m(\delta_e)), \\ C_T = \begin{cases} 0.02576\phi, & \text{if } \phi < 1, \\ 0.0224 + 0.00336\phi, & \text{if } \phi \geq 1, \end{cases} \end{cases} \tag{2}$$

where ϕ and δ_e are throttle setting and elevator deflection; C_L, C_D, C_T, and C_m represent lift, drag, thrust, and pitching moment coefficient of AHV; and ρ and s are air density and reference area of the aircraft wing, respectively [27].

2.2. Model Transformation. In order to apply the backstepping method, the longitudinal dynamics of AHV need to be transformed into a strict feedback form as follows:

$$\begin{cases} \dot{V} = g_V\phi + f_V + d_V, \\ \dot{h} \approx V\gamma, \\ \dot{\gamma} = g_\gamma\theta + f_\gamma + d_\gamma, \\ \dot{\theta} = q, \\ \dot{q} = g_q\delta_e + f_q + d_q, \end{cases} \tag{3}$$

where

$$\begin{cases} g_V = \dfrac{1}{2}\dfrac{\rho V^2 S C_{T,\phi}(\alpha)\cos\alpha}{m}, \\ g_\gamma = \dfrac{1}{2}\dfrac{\rho V^2 S C_L}{mV}, \\ g_q = \dfrac{1}{2}\dfrac{\rho V^2 S\bar{c}C_M^{\delta_e}}{I_{yy}}, \\ f_V = \dfrac{1}{2}\dfrac{\rho V^2 S(C_T(\alpha)\cos\alpha - C_D)}{m} - g\sin\gamma, \\ f_\gamma = \dfrac{1}{2}\dfrac{\rho V^2 S\left(C_L + C_{T,\phi}(\alpha)\phi\sin\alpha + C_T\alpha\sin\alpha - C_L^\alpha\gamma\right)}{mV} - \dfrac{g\cos\gamma}{V}, \\ f_q = \dfrac{1}{2}\dfrac{\rho V^2 S\left(\bar{c}C_M^{\delta_e}\delta_e\right)}{I_{yy}}. \end{cases} \tag{4}$$

Assumption 1. The uncertainties $d_i(i = V, \gamma, q)$ are continuously differentiable and satisfy $|\dot{d}_i| \leq \sigma_i$, in which σ_i are unknown positive constants.

Remark 2. Assumption 1 is reasonable because the main disturbances of large amplitude usually have low frequencies. Similar assumptions are also presented in [28, 29].

3. Controller Design

In this section, the control system based on the backstepping sliding mode control method is introduced for the AHV model to achieve altitude and velocity command tracking control. The control diagram is shown in Figure 2. Velocity tracking and altitude tracking controller are designed separately. The control objective is to track the desired velocity and altitude commands by adjusting the control input Φ and δ_e. The altitude subsystem is a four-order dynamic system as shown in (3). The backstepping method is used to divide the altitude control subsystem into several first-order subsystems. Then, controllers based on the adaptive supertwisting sliding mode control method are designed for each subsystem, to obtain temporary virtual control variables and final control outputs. The stability of a closed system can be verified by the Lyapunov approach.

3.1. Adaptive Supertwisting Sliding Mode Control Algorithm. Compared with the traditional supertwisting sliding mode algorithm [30], the novel algorithm [17] has the following advantages: the new algorithm does not need the information of the upper bound of external disturbances, which is needed in traditional sliding mode methods; the adaption of controller gain parameters is helpful to avoid the chattering phenomenon. These advantages make it suitable for AHV control, because there are kinds of parameter uncertainties in the AHV modelling process, and it is difficult to obtain the upper bound of the atmospheric disturbance.

Consider the following first-order nonlinear system:

$$\dot{x} = f(x) + g(x)u, \tag{5}$$

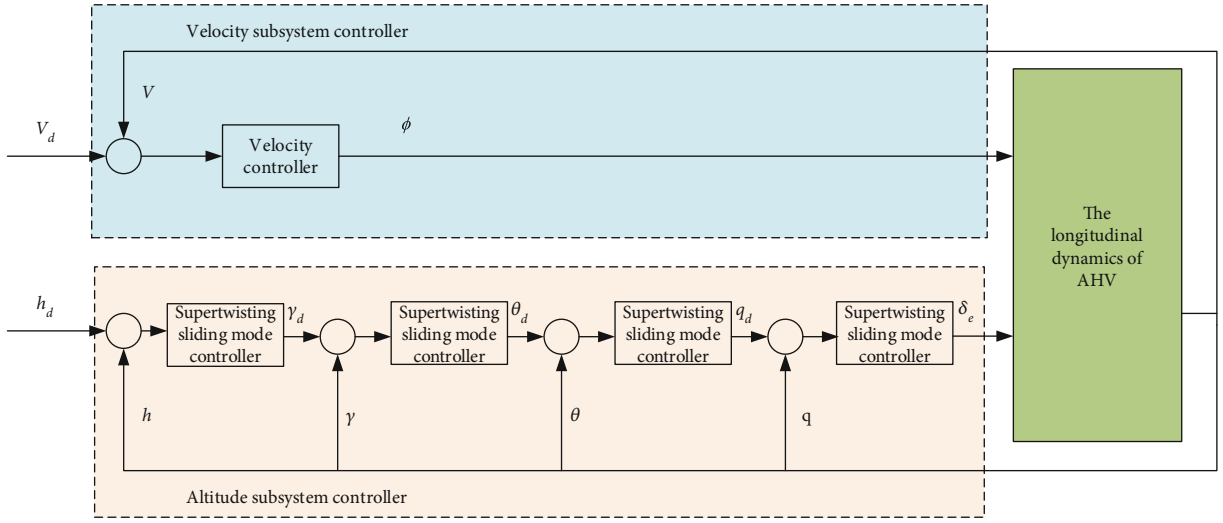

Figure 2: Block diagram of the proposed controller of AHV.

where x is the system state variable, as the system output; $f(x)$ is a known function of the system state; and u is the control input. The reaching law ω of the traditional supertwisting sliding mode controller is given as follows [30]:

$$\begin{cases} \omega = -\lambda |s|^{0.5} \text{ sign } (s) + v, \\ \dot{v} = -\dfrac{\beta}{2} \text{ sign } (s). \end{cases} \tag{6}$$

The feature of the supertwisting sliding mode algorithm is that it only needs the information of sliding mode variable s. The algorithm can be directly applied to the first-order nonlinear system without introducing other control variables.

The parameters λ and β in (6) are constant and need to be set in advance. Normally, these parameters are selected large enough to ensure the robustness of the control system. However, when the external disturbance is small, the large control gain parameter may lead to actuator chattering. The control structure in this paper is consistent with the traditional supertwisting algorithm (6). The parameters λ, β are generated by the adaptive law (7) used in [17], and the control gains can change with external disturbances:

$$\begin{cases} \dot{\lambda} = \begin{cases} \omega_1 \sqrt{\dfrac{\gamma_1}{2}} \text{ sign } (|s| - \mu), & \text{if } \lambda > \lambda_m, \\ \eta, & \text{if } \lambda \le \lambda_m, \end{cases} \\ \beta = 2\varepsilon\lambda, \end{cases} \tag{7}$$

where $\varepsilon, \gamma_1, \omega_1, \eta$ are positive constants greater than zero and λ_m is a small positive constant.

The adaptive supertwisting sliding mode control algorithm is used in the next section, to get the virtual control variables and final control inputs.

3.2. Altitude Controller Design

Step 1. The tracking error of altitude is defined as $e_h = h - h_d$, where h_d represents the altitude command, and then, $\dot{e}_h \approx V\gamma - \dot{h}_d$. Define the sliding mode variable as $S_h = e_h$. The $h - \gamma$ subsystem is a first-order system, and therefore, the supertwisting sliding mode controller (6) can be applied to it. The virtual control input γ_d is designed as

$$\begin{cases} \gamma_d = \dfrac{1}{V}\left(-\lambda_h |e_h|^{0.5} \text{ sign } (S_h) + u_h + \dot{h}_d\right), \\ \dot{u}_h = -a_h \text{ sign } (S_h), \end{cases} \tag{8}$$

where λ_h and a_h can be calculated using adaptive law (9):

$$\begin{cases} \dot{\lambda}_i = \begin{cases} \omega_i \sqrt{\dfrac{\gamma_i}{2}} \text{ sign } (|S_i| - \mu_i), & \text{if } \lambda_i > \lambda_{m,i}, \\ \eta_i, & \text{if } \lambda_i \le \lambda_{m,i}, \end{cases} \\ a_i = 2\varepsilon_i \lambda_i, \end{cases} \tag{9}$$

where $i = h, \gamma, \theta, q, V$.

Step 2. In order to obtain the virtual control input of θ_d, the differential of γ_d is needed. However, it is difficult to get the accurate differential of γ_d in (8).

To avoid the "explosion of terms" problem in the backstepping design, the dynamic surface control technology is adopted. The first-order low-pass filter is used to obtain the derivatives of virtual control variables. The form of the first-order low-pass filter is

$$\begin{cases} \tau_i \dot{\bar{x}}_i + \bar{x}_i = x_i, \\ \bar{x}_i(0) = x_i(0), \end{cases} \tag{10}$$

where τ_1 is the time constant of the low-pass filter and x_i is the input of the filter. $\dot{\bar{\gamma}}_d$ can be obtained by inputting γ_d into (10).

Define the error of path angle $e_\gamma = \gamma - \gamma_d$. Select e_γ as the sliding mode variable ($S_\gamma = e_\gamma$). The virtual control input of θ_d is given as

$$\begin{cases} \theta_d = \dfrac{1}{g_\gamma}\left(\dot{\bar{\gamma}}_d - f_\gamma - \lambda_\gamma |e_\gamma|^{0.5} \operatorname{sign}(S_\gamma) + u_\gamma\right), \\ \dot{u}_\gamma = -a_\gamma \operatorname{sign}(S_\gamma), \end{cases} \tag{11}$$

where λ_γ and a_γ are obtained through adaptive law (9).

Step 3. Define the error of pitch angle $e_\theta = \theta - \theta_d$, where θ_d is obtained by Step 2. Let $S_\theta = e_\theta$, and then, the virtual control input of q_d is given as

$$\begin{cases} q_d = -\lambda_\theta |S_\theta|^{0.5} \operatorname{sign}(S_\theta) + u_\theta + \dot{\bar{\theta}}_d, \\ \dot{u}_\theta = -a_\theta \operatorname{sign}(S_\theta), \end{cases} \tag{12}$$

where λ_θ and a_θ are obtained through adaptive law (9); $\dot{\bar{\theta}}_d$ is obtained by inputting θ_d into (10).

Step 4. Define the error of pitching angle rate $e_q = q - q_d$. Let $S_q = e_q$; then, the actual control input of δ_e is given as

$$\begin{cases} \delta_e = \dfrac{1}{g_q}\left(-f_q - \lambda_q |S_q|^{0.5} \operatorname{sign}(S_q) + u_q + \dot{\bar{q}}_d\right), \\ \dot{u}_q = -a_q \operatorname{sign}(S_q), \end{cases} \tag{13}$$

where λ_q and a_q are obtained through adaptive law (9), and $\dot{\bar{q}}_d$ is obtained by inputting q_d into (10).

3.3. Velocity Controller Design. In the longitudinal dynamic model (3) of AHV, the velocity subsystem is a first-order nonlinear system; therefore, the adaptive supertwisting sliding mode algorithm can be directly used in velocity control.

Define the velocity tracking error as $e_V = V - V_d$, where V_d is the velocity command signal. The differential of e_V is given as $\dot{e}_V = g_V\phi + f_V + d_V - \dot{V}_d$. In order to eliminate the steady-state error of velocity, the sliding mode variable is selected as $S_V = \int_0^t e_V dt + e_V$.

The control input is given as

$$\begin{cases} \phi = \dfrac{1}{g_V}\left(-f_V - e_V + \dot{V}_d - \lambda_V |S_V|^{1/2} \operatorname{sign}(S_V) + u_V\right), \\ \dot{u}_V = -a_V \operatorname{sign}(S_V), \end{cases} \tag{14}$$

where λ_V and a_V are obtained through adaptive law (9).

4. Stability Analysis

In this section, the stability of the proposed controller is analysed by the Lyapunov theory. Define the Lyapunov function as

$$V_l = \frac{1}{2}S_V^2 + \frac{1}{2}S_h^2 + \frac{1}{2}S_\gamma^2 + \frac{1}{2}S_\theta^2 + \frac{1}{2}S_q^2. \tag{15}$$

The differential of (15) is

$$\dot{V}_l = S_V\dot{S}_V + S_h\dot{S}_h + S_\gamma\dot{S}_\gamma + S_\theta\dot{S}_\theta + S_q\dot{S}_q, \tag{16}$$

$$\begin{aligned} \dot{V}_l = {} & S_V\left(e_V + \dot{V} - \dot{V}_d\right) + S_h\left(\dot{h} - \dot{h}_d\right) + S_\gamma(\dot{\gamma} - \dot{\gamma}_d) \\ & + S_\theta\left(\dot{\theta} - \dot{\theta}_d\right) + S_q(\dot{q} - \dot{q}_d). \end{aligned} \tag{17}$$

Substituting (3) into equation (17), we can get

$$\begin{aligned} \dot{V}_l = {} & S_V\left(e_V + g_V\phi + f_V + d_V - \dot{V}_d\right) + S_h\left(V\gamma - \dot{h}_d\right) \\ & + S_\gamma\left(g_\gamma\theta + f_\gamma + d_\gamma - \dot{\gamma}_d\right) + S_\theta\left(q - \dot{\theta}_d\right) \\ & + S_q\left(g_q\delta_e + f_q + d_q - \dot{q}_d\right). \end{aligned} \tag{18}$$

Substituting (8), (11), (12), (13), and (14) into equation (18), we have

$$\begin{aligned} \dot{V}_l = {} & S_V\left(-\lambda_V |S_V|^{0.5} \operatorname{sign}(S_V) + u_V + d_V\right) \\ & + S_h\left(-\lambda_h |S_h|^{0.5} \operatorname{sign}(S_h) + u_h\right) + S_\gamma\left(-\lambda_\gamma |S_\gamma|^{0.5} \operatorname{sign}(S_\gamma)\right. \\ & \left. + u_\gamma + d_\gamma + \Delta_{\dot{\gamma}_d}\right) + S_\theta\left(-\lambda_\theta |S_\theta|^{0.5} \operatorname{sign}(S_\theta) + u_\theta + \Delta_{\dot{\theta}_d}\right) \\ & + S_q\left(-\lambda_q |S_q|^{0.5} \operatorname{sign}(S_q) + u_q + d_q + \Delta_{\dot{q}_d}\right), \end{aligned} \tag{19}$$

where $\Delta_{\dot{\gamma}_d} = \dot{\bar{\gamma}}_d - \dot{\gamma}_d$, $\Delta_{\dot{\theta}_d} = \dot{\bar{\theta}}_d - \dot{\theta}_d$, and $\Delta_{\dot{q}_d} = \dot{\bar{q}}_d - \dot{q}_d$. Then, (19) can be rewritten as

$$\begin{aligned} \dot{V}_l = {} & -\lambda_V |S_V|^{0.5} |S_V| + S_V(u_V + d_V) - \lambda_h |S_h|^{0.5} |S_h| + S_h u_h \\ & - \lambda_\gamma |S_\gamma|^{0.5} |S_\gamma| + S_\gamma(u_\gamma + d_\gamma) - \lambda_\theta |S_\theta|^{0.5} |S_\theta| + S_\theta u_\theta \\ & - \lambda_q |S_q|^{0.5} |S_q| + S_q(u_q + d_q) + S_\gamma\Delta_{\dot{\gamma}_d} + S_\theta\Delta_{\dot{\theta}_d} + S_q\Delta_{\dot{q}_d}. \end{aligned} \tag{20}$$

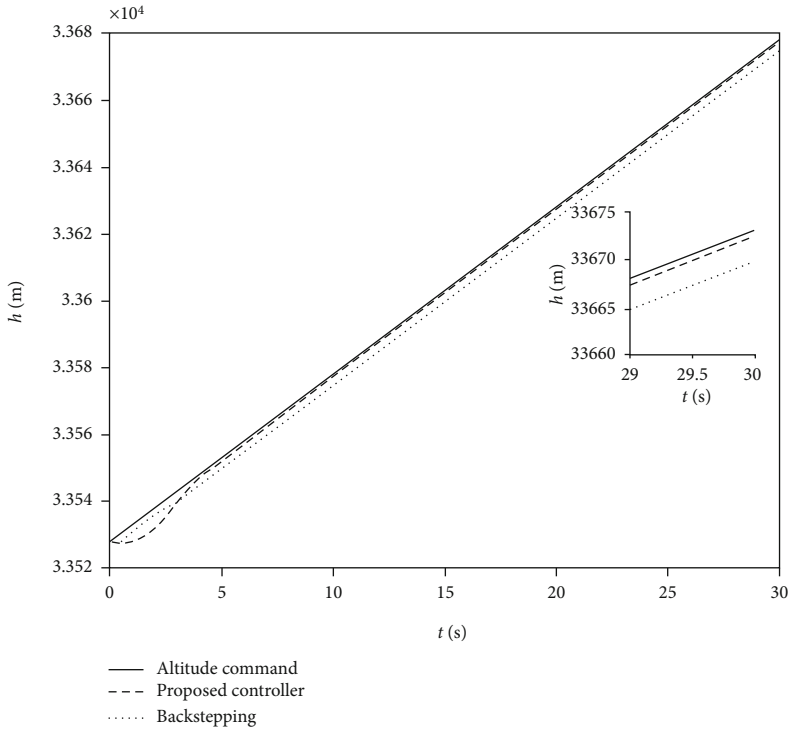

Figure 3: Altitude tracking.

Substituting (8), (11), (12), (13), and (14) into equation (20), we can get

$$\begin{aligned}\dot{V}_l \le & -\lambda_V |S_V|^{0.5} |S_V| - \lambda_h |S_h|^{0.5} |S_h| - \lambda_\gamma |S_\gamma|^{0.5} |S_\gamma| \\ & - \lambda_\theta |S_\theta|^{0.5} |S_\theta| - \lambda_q |S_q|^{0.5} |S_q| + S_V \int_0^t -\bar{a}_V \operatorname{sign}(S_V) dt \\ & + S_h \int_0^t -a_h \operatorname{sign}(S_h) dt + S_\gamma \int_0^t -\bar{a}_\gamma \operatorname{sign}(S_\gamma) dt + S_\theta \int_0^t \\ & - a_\theta \operatorname{sign}(S_\theta) dt + S_q \int_0^t -\bar{a}_q \operatorname{sign}(S_q) dt + S_\gamma \Delta_{\dot{\gamma}_d} \\ & + S_\theta \Delta_{\dot{\theta}_d} + S_q \Delta_{\dot{q}_d},\end{aligned} \tag{21}$$

where $\bar{a}_V = a_V - \sigma_V$, $\bar{a}_\gamma = a_\gamma - \sigma_\gamma$, and $\bar{a}_q = a_q - \sigma_q$. $\bar{a}_V$, $\bar{a}_\gamma$, and $\bar{a}_q$ are positive values according to Theorem 1 in [17].

According to Young's inequality, we have

$$\begin{aligned} S_\gamma \Delta_{\dot{\gamma}_d} &\le \frac{2}{3} |S_\gamma|^{1.5} + \frac{1}{3} \left|\Delta_{\dot{\gamma}_d}\right|^3, \\ S_\theta \Delta_{\dot{\theta}_d} &\le \frac{2}{3} |S_\theta|^{1.5} + \frac{1}{3} \left|\Delta_{\dot{\theta}_d}\right|^3, \\ S_q \Delta_{\dot{q}_d} &\le \frac{2}{3} |S_q|^{1.5} + \frac{1}{3} \left|\Delta_{\dot{q}_d}\right|^3. \end{aligned} \tag{22}$$

Then, (21) can be written as

$$\begin{aligned}\dot{V}_l \le & -\lambda_V |S_V|^{1.5} - \lambda_h |S_h|^{1.5} - \left(\lambda_\gamma - \frac{2}{3}\right) |S_\gamma|^{1.5} \\ & - \left(\lambda_\theta - \frac{2}{3}\right) |S_\theta|^{1.5} - \left(\lambda_q - \frac{2}{3}\right) |S_q|^{1.5} + \int_0^t -\bar{a}_V |S_V| dt \\ & + \int_0^t -a_h |S_h| dt + \int_0^t -\bar{a}_\gamma |S_\gamma| dt + \int_0^t -a_\theta |S_\theta| dt + \int_0^t \\ & - \bar{a}_q |S_q| dt + \frac{1}{3} \left|\Delta_{\dot{\gamma}_d}\right|^3 + \frac{1}{3} \left|\Delta_{\dot{\theta}_d}\right|^3 + \frac{1}{3} \left|\Delta_{\dot{q}_d}\right|^3.\end{aligned} \tag{23}$$

According to the following inequality

$$\left(\sum_{i=1}^n |x_i|\right)^p \le \sum_{i=1}^n |x_i|^p, \tag{24}$$

where $0 < p < 1$, it can be obtained that

$$\begin{aligned} V_l^{0.75} \le & \frac{1}{2^{0.75}} |S_V|^{1.5} + \frac{1}{2^{0.75}} |S_h|^{1.5} + \frac{1}{2^{0.75}} |S_\gamma|^{1.5} + \frac{1}{2^{0.75}} |S_\theta|^{1.5} \\ & + \frac{1}{2^{0.75}} |S_q|^{1.5}. \end{aligned} \tag{25}$$

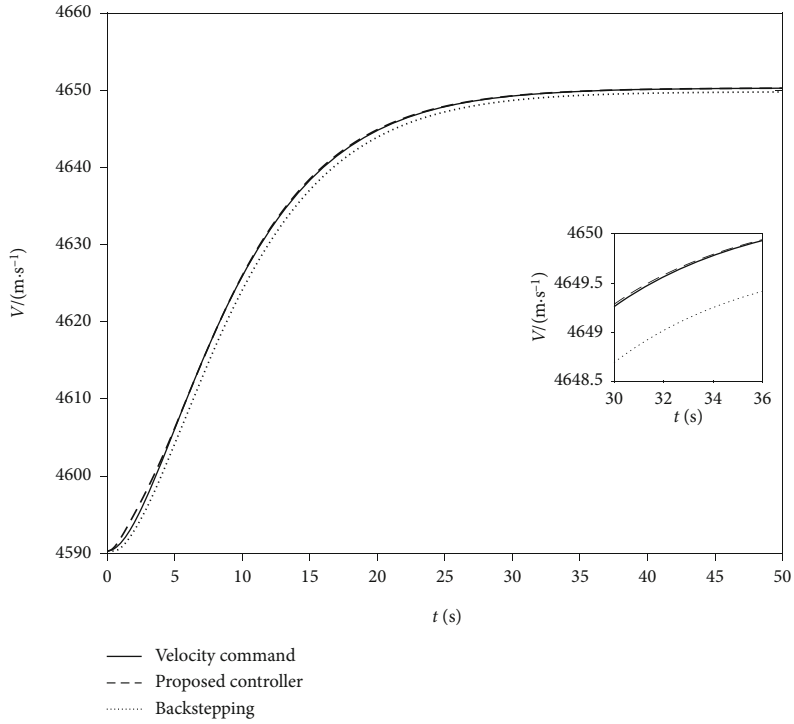

Figure 4: Velocity tracking.

Applying (25) to (23), we have

$$\dot{V}_l \le -\lambda_V |S_V|^{1.5} - \lambda_h |S_h|^{1.5} - \left(\lambda_\gamma - \frac{2}{3}\right)|S_\gamma|^{1.5} - \left(\lambda_\theta - \frac{2}{3}\right)|S_\theta|^{1.5} - \left(\lambda_q - \frac{2}{3}\right)|S_q|^{1.5} + \frac{1}{3}\left|\Delta_{\dot{\gamma}_d}\right|^3 + \frac{1}{3}\left|\Delta_{\dot{\theta}_d}\right|^3 + \frac{1}{3}\left|\Delta_{\dot{q}_d}\right|^3 \le -kV_l^{0.75} + \sigma, \quad (26)$$

where

$$k = \min\left\{2^{0.75}\lambda_V, 2^{0.75}\lambda_h, 2^{0.75}\left(\lambda_\gamma - \frac{2}{3}\right), 2^{0.75}\left(\lambda_\theta - \frac{2}{3}\right), 2^{0.75}\left(\lambda_q - \frac{2}{3}\right)\right\},$$

$$\sigma = \frac{1}{3}\left|\Delta_{\dot{\gamma}_d}\right|^3 + \frac{1}{3}\left|\Delta_{\dot{\theta}_d}\right|^3 + \frac{1}{3}\left|\Delta_{\dot{q}_d}\right|^3. \quad (27)$$

According to Lemma 2 in [31] and Lemma 3.6 in [32], the closed-loop system is finite-time bounded. And the convergence time is $t_c \le V_l^{0.25}(x(0))/0.75k\theta_0$; the error converges into $\Omega = \{X \mid V_l^{0.75} \le \sigma/k(1-\theta_0)\}$ when $t \ge t_c$, where $0 < \theta_0 < 1$ and $x = [S_V, S_h, S_\gamma, S_\theta, S_q]^T$.

Remark 3. The value of σ mainly depends on the error of low-pass filters (10); in general, these errors are small because the time constant of filters is small enough.

5. Simulation Results

In this section, simulation tests are conducted to demonstrate the performance of the controller proposed in this paper. The main simulation settings in this paper are as follows.

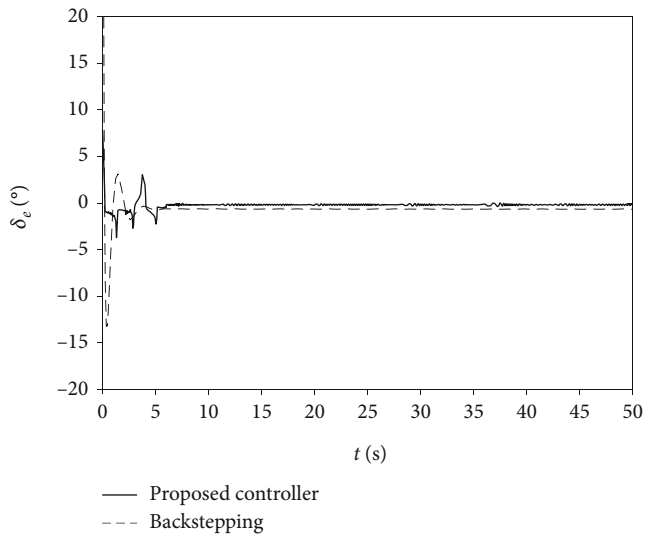

Figure 5: Elevator deflection.

5.1. Initial Condition and Command Signal. The initial state of AHV is the following: velocity 4590 m/s, height 33528 m, angle of attack 2.745°, and pitch rate 0 rad/s. The altitude command signal is climbing at speed of 5 m/s, and the velocity command increased flight speed from 4590 m/s to 4610 m/s. A filter is used on velocity command to avoid a sharp change of throttle. The filter is set as $0.2^2/(s^2 + 2 \cdot 0.2s + 0.2^2)$.

5.2. Parameter Uncertainties. In order to verify the robust performance of the proposed controller, model parameter perturbations are considered in the simulation including

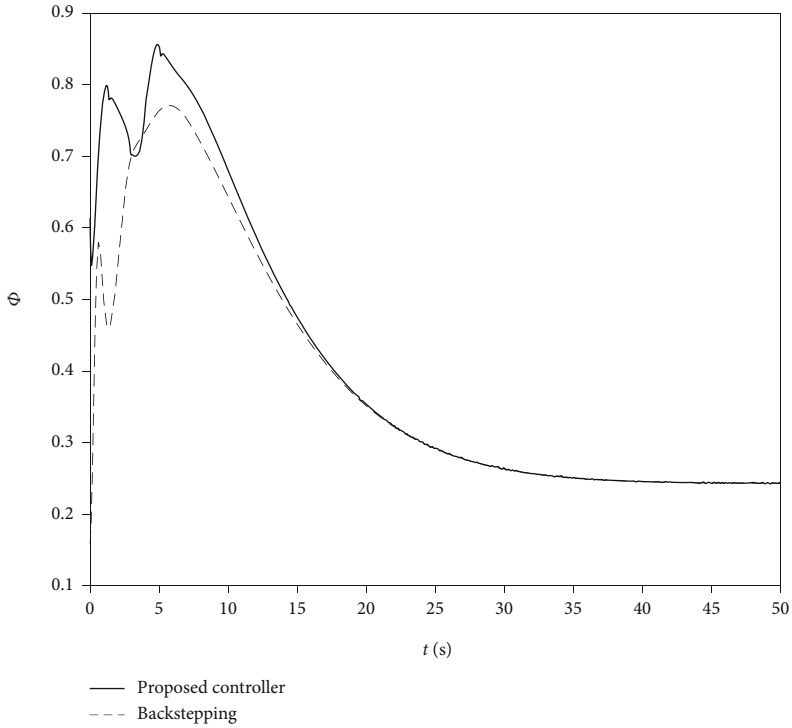

Figure 6: Throttle setting.

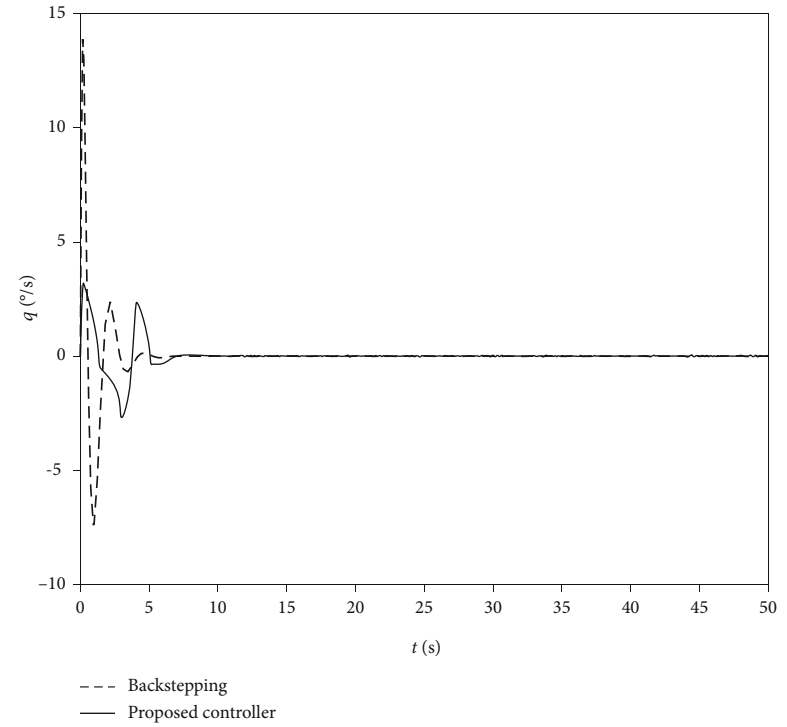

Figure 7: Pitching angle rate.

aircraft mass, wing reference area, aspect ratio, air density, gravity acceleration, lift coefficient, drag coefficient, and pitching moment coefficient. The value of these parameters varies by 10%.

5.3. Control Parameters. The value of λ in (6) determines that the value of γ_1, ω_1 in adaptive law (7) affects the controller sensitivity to parameter perturbations or external disturbances. If these parameters are too large, they may

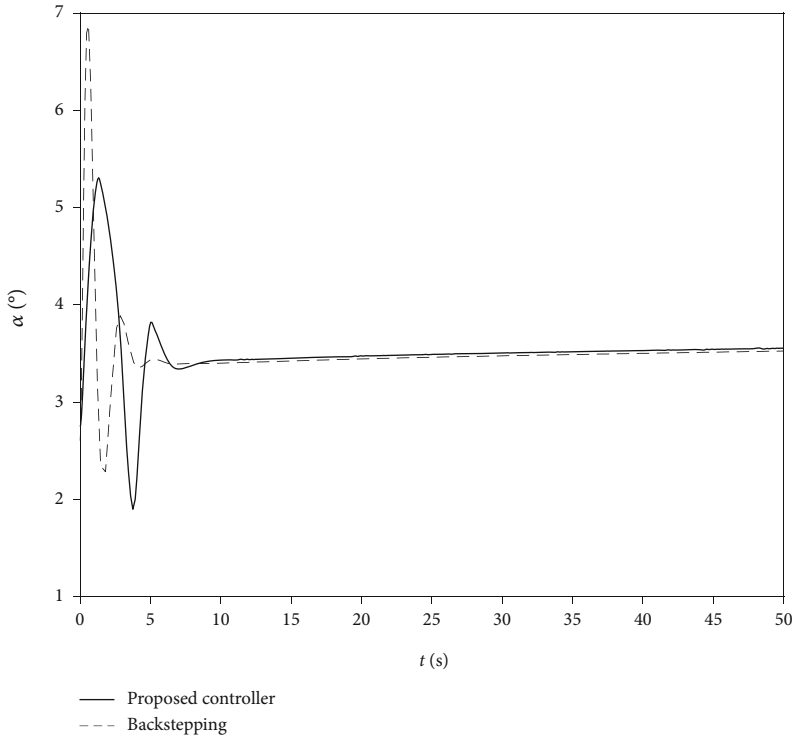

Figure 8: Attack angle.

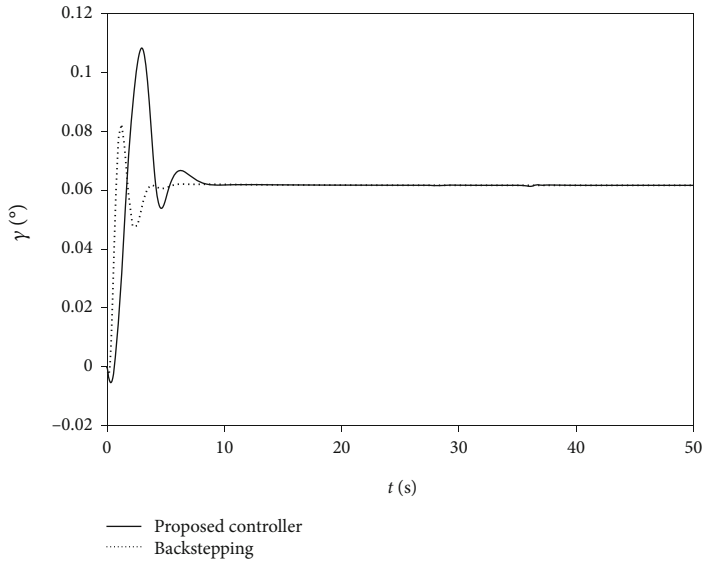

Figure 9: Path angle.

cause a chattering problem. The parameters in this paper are selected as $\omega_q = 0.5, \gamma_q = 0.05, \mu_q = 0.01$; $\omega_h = 0.1, \gamma_h = 0.01, \mu_h = 0.002$; and $\omega_h = 0.3, \gamma_h = 0.05, \mu_h = 0.01$.

The proposed controller was applied to the longitudinal model with the simulation toolbox of MATLAB.

In order to verify the performance of the proposed controller, a comparison simulation experiment is carried out in this paper; the controller based on backstepping combined with the dynamic surface control method is taken into account.

The tracking curve of altitude and velocity simulation results is shown in Figures 3 and 4, respectively. The control inputs of the elevator and throttle setting are shown in Figures 5 and 6, respectively. Figures 7–9 represent the pitching rate, attack angle, and path angle.

It can be observed in Figure 3 that there are some errors between the altitude command and actual altitude controlled by the proposed controller during the first 5 seconds. The altitude error of the backstepping controller is better during the first 5 seconds. However, it is obvious that the altitude error

of the proposed controller converges to a very small value from the 10th second to the end, while there is always an error of altitude of the backstepping controller, which means that the proposed controller has better performance in dealing with uncertainties than the traditional backstepping method.

As shown in Figure 4, both controllers have good performances in velocity tracking control, but the final velocity error of the proposed controller is smaller.

As shown in Figure 5, the elevator deflection of the proposed controller changes greatly in the first 5 seconds; to eliminate the altitude error, then, in the later stage of simulation, it keeps small with acceptable fluctuation due to external disturbances and parameter perturbation.

It is shown in Figure 6 that the throttle command of both controllers increases rapidly during 0-10 seconds because of velocity command changes. After about 40 seconds, the throttle command converges to a constant value, in order to produce a constant thrust to counteract air drag to fly at a constant speed.

It is shown in Figures 7–9 that the pitching rate, attack angle, and path angle of both controllers are acceptable.

6. Conclusions

In this paper, a controller combining the backstepping method and adaptive supertwisting sliding mode control algorithm is proposed to solve the problem of altitude and velocity tracking control of AHV with parameter uncertainties and disturbances. In order to use the proposed control method, the AHV model needs to be transformed into a strict feedback form, and then, the high-order control problem of AHV can be divided into several first-order subsystems. The stability of the proposed control system is theoretically analysed. The simulation results show that the adaptive backstepping sliding mode controller has strong robust performance and can realize the precise and fast tracking control of the altitude and velocity of AHV. The further improvement of the adaptive law of parameters in the supertwisting sliding mode algorithm could be studied in future work.

Data Availability

The data used to support the findings of this study are available from the corresponding author upon request.

Conflicts of Interest

The authors declare that there is no conflict of interest regarding the publication of this paper.

Acknowledgments

This work was supported by the National Natural Science Foundation of China under grant 61673209.

References

[1] B. Xu and Z. K. Shi, "An overview on flight dynamics and control approaches for hypersonic vehicles," *Science China-Information Sciences*, vol. 58, no. 7, pp. 1–19, 2015.

[2] F. Baris, M. Maj, and I. Petros, "Flight dynamics and control of air-breathing hypersonic vehicles: review and new directions," in *12th AIAA International Space Planes and Hypersonic Systems and Technologies*, Norfolk, Virginia, 2003.

[3] M. A. Bolender, "An overview on dynamics and controls modelling of hypersonic vehicles," in *2009 American control conference*, pp. 2507–2512, St. Louis, MO, USA, 2009.

[4] J. D. Shaughnessy, S. Z. Pinckney, J. D. Mcminn, C. I. Cruz, and M.-L. Kelley, *Hypersonic Vehicle Simulation Model: Winged-Cone Configuration*, NASA Langley Research Center, 1990, TM-102610.

[5] X. Y. Tao, N. Li, and S. Y. Li, "Multiple model predictive control for large envelope flight of hypersonic vehicle systems," *Information Sciences*, vol. 328, no. 328, pp. 115–126, 2016.

[6] L. X. Zhang, L. Nie, B. Cai, S. Yuan, and D. Z. Wang, "Switched linear parameter-varying modeling and tracking control for flexible hypersonic vehicle," *Aerospace Science and Technology*, vol. 95, article 105445, 2019.

[7] W. W. Qin, H. Bing, L. Gang, and P. T. Zhao, "Robust model predictive tracking control of hypersonic vehicles in the presence of actuator constraints and input delays," *Journal of the Franklin Institute-Engineering and Applied Mathematics*, vol. 353, no. 17, pp. 4351–4367, 2016.

[8] J. Zhang, C. Sun, R. Zhang, and C. Qian, "Adaptive sliding mode control for re-entry attitude of near space hypersonic vehicle based on backstepping design," *IEEE/CAA Journal of Automatica Sinica*, vol. 2, no. 1, pp. 94–101, 2015.

[9] H. J. Xu, M. D. Mirmirani, and P. A. Ioannou, "Adaptive sliding mode control design for a hypersonic flight vehicle," *Journal of Guidance Control and Dynamics*, vol. 27, no. 5, pp. 829–838, 2004.

[10] Q. L. Hu and Y. Meng, "Adaptive backstepping control for air-breathing hypersonic vehicle with actuator dynamics," *Aerospace Science and Technology*, vol. 67, pp. 412–421, 2017.

[11] Z. Guo, J. Chang, J. Guo, and J. Zhou, "Adaptive twisting sliding mode algorithm for hypersonic reentry vehicle attitude control based on finite-time observer," *ISA Transactions*, vol. 77, pp. 20–29, 2018.

[12] H. An, Q. Wu, C. Wang, and X. Cao, "Simplified fault-tolerant adaptive control of air-breathing hypersonic vehicles," *International Journal of Control*, vol. 82-83, pp. 312–322, 2020.

[13] Z. Y. Guo, Q. W. Ma, J. G. Guo, B. Zhao, and J. Zhou, "Performance-involved coupling effect-triggered scheme for robust attitude control of HRV," *IEEE/ASME Transactions on Mechatronics*, vol. 23, pp. 1288–1298, 2020.

[14] Y. Wang, X. Yang, and H. Yan, "Reliable fuzzy tracking control of near-space hypersonic vehicle using aperiodic measurement information," *IEEE Transactions on Industrial Electronics*, vol. 66, no. 12, pp. 9439–9447, 2019.

[15] H. An, Q. Wu, C. Wang, and X. Cao, "Scramjet operation guaranteed longitudinal control of air-breathing hypersonic vehicles," *IEEE/ASME Transactions on Mechatronics*, p. 1, 2020.

[16] B. Lu, Y. Fang, and N. Sun, "Sliding mode control for underactuated overhead cranes suffering from both matched and unmatched disturbances," *Mechatronics*, vol. 47, pp. 116–125, 2017.

[17] Y. Shtessel, M. Taleb, and F. Plestan, "A novel adaptive-gain supertwisting sliding mode controller: methodology and application," *Automatica*, vol. 48, no. 5, pp. 759–769, 2012.

[18] P. V. Kokotovic, M. Krstic, and I. Kanellakopoulos, "Backstepping to passivity: recursive design of adaptive systems," in *Proceedings of the 31st IEEE Conference on Decision and Control*, vol. 1-4, pp. 3276–3280, Tucson, AZ, USA, 1992.

[19] D. Swaroop, J. K. Hedrick, P. P. Yip, and J. C. Gerdes, "Dynamic surface control for a class of nonlinear systems," *IEEE Transactions on Automatic Control*, vol. 45, no. 10, pp. 1893–1899, 2000.

[20] X. Bu, X. Wu, R. Zhang, Z. Ma, and J. Huang, "Tracking differentiator design for the robust backstepping control of a flexible air-breathing hypersonic vehicle," *Journal of the Franklin Institute*, vol. 352, no. 4, pp. 1739–1765, 2015.

[21] L. Fiorentini, A. Serrani, M. A. Bolender, and D. B. Doman, "Nonlinear robust adaptive control of flexible air-breathing hypersonic vehicles," *Journal of Guidance Control and Dynamics*, vol. 32, no. 2, pp. 402–417, 2009.

[22] B. J. Bialy, J. Klotz, J. W. Curtis, and W. E. Dixon, "An adaptive backstepping controller for a hypersonic air-breathing missile," in *AIAA Guidance, Navigation, and Control Conference*, Minneapolis, Minnesota, 2012.

[23] H. Li and L. H. Dou, "Adaptive backstepping non-singular fast terminal sliding mode control for mismatched uncertain systems," *Control & Decision*, vol. 27, no. 10, 2012.

[24] X. Wang, J. Guo, S. Tang, and S. Qi, "Fixed-time disturbance observer based fixed-time back-stepping control for an air-breathing hypersonic vehicle," *ISA Transactions*, vol. 88, pp. 233–245, 2019.

[25] A. Estrada, L. Fridman, and R. Iriarte, "Combined backstepping and HOSM control design for a class of nonlinear MIMO systems," *International Journal of Robust and Nonlinear Control*, vol. 27, no. 4, pp. 566–581, 2017.

[26] Y. Xia, Z. Zhu, and M. Fu, "Back-stepping sliding mode control for missile systems based on an extended state observer," *IET Control Theory & Applications*, vol. 5, no. 1, pp. 93–102, 2011.

[27] X. Jiao, B. Fidan, J. Jiang, and M. Kamel, "Adaptive mode switching of hypersonic morphing aircraft based on type-2 TSK fuzzy sliding mode control," *Science China-Information Sciences*, vol. 58, no. 7, pp. 1–15, 2015.

[28] S. Marco, E. Mooij, and S. Theil, "Adaptive disturbance-based high-order sliding-mode control for hypersonic-entry vehicles," *Journal of Guidance, Control, and Dynamics*, vol. 40, no. 3, pp. 521–536, 2017.

[29] Y. Xi and Y. Meng, "Adaptive actuator failure compensation control for hypersonic vehicle with full state constraints," *Aerospace Science and Technology*, vol. 85, pp. 464–473, 2019.

[30] A. Levant, "Sliding order and sliding accuracy in sliding mode control," *International Journal of Control*, vol. 58, no. 6, pp. 1247–1263, 1993.

[31] H. Min, S. Xu, J. Gu, and Z. Zhang, "Adaptive finite-time stabilization of nonlinearly parameterized systems subject to mismatching disturbances," *International Journal of Robust and Nonlinear Control*, vol. 29, no. 11, pp. 3469–3484, 2019.

[32] Z. Zhu, Y. Xia, and M. Fu, "Attitude stabilization of rigid spacecraft with finite-time convergence," *International Journal of Robust and Nonlinear Control*, vol. 21, no. 6, pp. 686–702, 2011.